

## Real-Time Diagnosis of Incipient Multiple Faults with Application for Kori Nuclear Power Plant

Hak Yeong Chung

Korea Electric Power Corporation

Zeungnam Bien

Korea Advanced Institute of Science and Technology

(Received January 27, 1995)

### 초기 다중고장 실시간 진단기법 개발 및 고리원전 적용

정학영

한국전력공사

변증남

한국과학기술원

(1995. 1. 27 접수)

### Abstract

This paper provides an improvement on our previous study [1] for multi-fault diagnosis in real time in large-scale systems. In the method, fault propagation probability(FPP) and fault propagation time(FPT) in a fuzzy sense are additively used to describe the fault propagation model(FPM) in more practical manner. A modified fault diagnosis procedure is also given. This method is applied for diagnosis of the primary system in the Kori nuclear power plant unit 2 under a transient condition in case of unit value of FPP on each branch of the FPM.

### 요 약

본 논문의 저자는 원자력 발전소와 같은 복잡한 대규모의 시스템의 실시간 고장진단 방법을 1994년 IEEE TNS Vol. 41, No. 4 호[1]에 발표하였다. 이번 논문에서는 고장전파모델(FPM)로서 같은 'Timed SDG Model'를 사용하고 있으나 고장전파시간(FPT)을 에메논리 개념을 이용하여 정확하게 구하기 어려운 FPT를 실질적으로 이용할수 있도록 했으며, 또한 고장전파확률(FPP)개념을 도입하여 하나이상의 고장원인 절점(Node)들을 절점고장율과 더불어, 보다 효과적으로 판별할수 있도록 했다. 또 FPM내에서 고장의 전파확률을 고려함으로써 보다 실질적인 고장 진단방법을 제시하였으며 본 제안된 방법을 고리 원전 2호기 1차계통에 적용하여 1차계통 FPM내의 각 FPP이 '1'인 경우에 한하여 그 성능을 입증하여 보았다.

## 1. Introduction

In a complex and large-scale systems such as nuclear power plants which are strongly nonlinear systems, signal validation is very important for proper plant surveillance, control, and safe operation. A good example of its relevance is a nuclear power plant, where after a fault tens of alarms can occur in a few seconds, which make it very difficult to locate the fault(s) origin when there is influx of abnormal signals because abnormal states in the plant are often detected at devices other than at the failed device (fault origin).

A number of useful technique for the automated fault diagnosis have been suggested in the literature [1-12]. Any technique for automated fault diagnosis may be classified into either as a quantitative method or as a qualitative one, depending on the rigor and precision of the used model. The quantitative fault diagnosis usually adopts a thermo-hydraulic mathematical model, and this method requires heavy computational load with extensive engineering manpower. The performance of model-based approaches depends strongly on the accuracy of the model. Every important dynamic characteristics should be included in the model. It must be able to handle changes in the operating point. If the model is not appropriate, the whole diagnostic system may fail to function properly. The sensitivity to modelling errors has become the key problem of the model-based methods[4].

The qualitative approach, on the other hand, is often capable of indentifying core knowledge of the process such as the variables and the signs of coefficients of the governing equations. The signed directed graph (SDG) is one of the most commonly used qualitative models to represent the causal effects between process variables. Nodes are used to represent the process variables or the process devices while branches are adopted to represent the influence between two adjacent nodes.

There are, however, some restrictions of the exist-

ing methods to real plant application due to (1) limited detection capability due to modelling error and computational load for the model-based diagnosis method[11], (2) the exact rule-derivation problem to avoid the spurious solutions for a rule-based fault diagnosis[3, 7, 9, 10], (3) a required large historical data treatment and no explanation capability ('How' and 'Why' functions) about the diagnosed results in case of artificial neural network(ANN)-based fault diagnosis[2, 4, 5, 8]. It is noted that there are some basic assumptions such as a single fault case, a single operating condition, and a steady-state condition in most existing fault diagnosis methods as described in the literature.

In this study an improved method is proposed by utilizing the signed directed graph(SDG) as fault propagation models (FPMs) with fault propagation time(FPT) and fault propagation probability(FPP) on each branch with feedback and feedforward control loops, ANNs capabilities such as non-linear mapping, classification, and a parallel computing capabilities, and together with a process knowledge-based system to eliminate spurious faults. The FPPs and fault rates of devices are used to evaluate the priority ranking among candidates of a fault origin.

The FPT can be obtained through plant operational data, expert knowledge, and the analysis including a computer simulation.

But it is not easy to get the exact value of each FPT in the timed SDG model, rather it is more practical to consider each FPT value as the value in a fuzzy sense. In this paper, the fuzzy concept is also introduced to calculate the FPT value for the real application.

The proposed method may solve the following issues which can be encountered in the real plant environment;

- (1) a large-scale system with many operating conditions
- (2) frequently a transient condition rather than a steady-state condition
- (3) multiple fault case as well as a single fault case

- (4) urgency of the early detection and diagnosis of fault, incipient fault(s) diagnosis.

This paper describes a fault propagation model, subsystem division, training data extraction, and fault diagnosis in sequence. Finally application to the Kori Nuclear Power Plant unit 2 is described.

## 2. Description of the Fault Propagation Model

A SDG model is commonly used for a FPM to represent the causal effects between process variables[9, 10]. The SDG in this work consists of nodes and branches with fuzzy FPTs and FPPs newly added on each branch. The nodes in the digraph represent the physical process variables or the process devices. The branches represent the causal relationships between them. The "qualitative state" of a process variable is defined to correspond to one of the three possible ranges, that is, low, normal, and high, which are sometimes represented simply as  $-1$ ,  $0$ , and  $+1$ , respectively.

The qualitative relationship between node  $A$  and  $A_j$  is described as follows:

$$\begin{array}{ccc} \bigcirc & \xrightarrow{\alpha_{ij}, t_{ij}, p_{ij}} & \bigcirc \\ A & & A_j \end{array} \quad (1)$$

Here  $\alpha_{ij}$  represents the  $\text{sign}(A \rightarrow A_j)$ ,  $t_{ij}$  the FPT, and  $p_{ij}$  the FPP from node  $A$  to node  $A_j$ .

In the sense of qualitative state, nodes take the value of high, normal, or low. For a typical sensor node  $A$ , the node  $A$  is expressed in the following form of deviation index[2]:

$$\begin{aligned} A &= \frac{\text{measured } A - \text{nominal } A}{\text{threshold for } A} \\ &= \frac{A_m - \bar{A}}{A_{st}} \end{aligned} \quad (2)$$

where  $A_m$  denotes the measured value of  $A$ ,  $\bar{A}$  the nominal value of  $A$ , and  $A_{st}$  the threshold value of  $A$ .

The value of  $A$  varies depending on the magnitude of three variables  $A_m$ ,  $\bar{A}$  and  $A_{st}$ . Also the value

of node  $A$  can be considered as a continuous value ranging from 'high' to 'low' in a quantitative manner.

The  $\text{sign}(A \rightarrow A_j) = '+'$  means that a positive (or negative) deviation in  $A$  leads to a positive (or negative) deviation in  $A_j$ . The values of  $\alpha_{ij}$  and  $t_{ij}$  can be obtained from operational experience, plant data, or the mathematical model. When the operational data or experience of operators are not sufficient to obtain the representation of a process, it is desirable to construct the SDG from the process model.

The process model is usually described by a set of ordinary equations (ODEs) and algebraic equations. If the model is given by a set of ODEs of the form,

$$dZ_i/dt = f(Z_1, Z_2, \dots, Z_n) \quad (3)$$

where  $Z_i$  is the state variable of the process, the causal relation of a branch in this case is defined to start from  $Z_i$  if  $(\partial f_i / \partial Z_i) \neq 0$  and the sign of  $(\partial f_i / \partial Z_i)$  is assigned to the branch.

In general, it may not be easy to get  $t_{ij}$  on each branch only from Eq (3), especially when there are coupled terms among the state variables in Eq (3). The  $t_{ij}$  in this case, can be estimated from the knowledge of the process characteristics and statistical data, which are acquired from the process and experienced experts. Also it may be obtained by simulating the process model depicted by ODEs. For the first-order lag system, for example, the time constant of the step input response can be considered as the fault propagation time of this system. Since the fault diagnosis is performed by applying the sensor patterns to the pre-trained ANNs, the fault propagation time,  $t_{ij}$ , is used to estimate the propagation time difference from the fault origin to various sensors which indicate final symptom to this fault node and to get the sensor patterns under transient conditions. It is remarked that the fault propagation time is not required for steady-state fault diagnosis.

### 2.1. Division into Subsystems

We propose that the system be divided into several

smaller subsystems so that each neural network takes charge of the fault diagnosis of each subsystem in real time with desirable efficiency. Specially, the whole system for fault diagnosis is hierarchically composed of the lower level modular-type neural networks and the top level supervisor (refer to Figure 1).

In general, some subsystems are physically inter-connected with each other while the fault diagnosis is performed at each subsystem independently. When a fault occurs in a subsystem, the fault can propagate to its adjacent subsystems that are connected to the faulty subsystem even though they are fault-free originally. These adjacent subsystems may be diagnosed as having faults and can declare the existence of faults. This kind of faults is called "spurious faults". The spurious faults, in this work, are removed at the top level supervisor using the knowledge on the inter-relation of the divided subsystems and the propagation time sequence of fault occurrence at each subsystem.

The size of a subsystem can be determined depending on the characteristics of the system and on the physical relationship among subsystems as well as in consideration of effectiveness in computation. It is

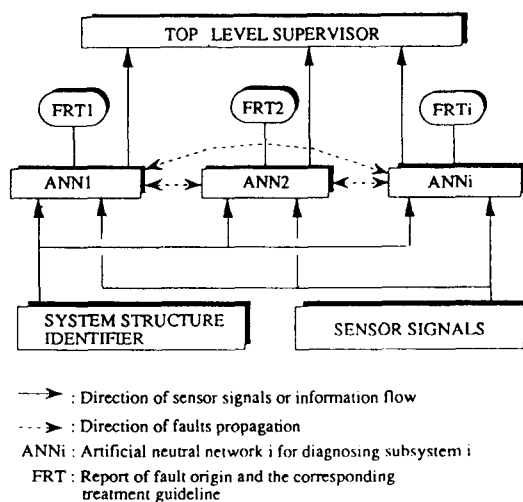


Fig. 1. Hierarchical Structure for Fault Diagnosis in a Large-scale System

desirable that any closed control loop should not be torn apart among subsystems but be included in a subsystem.

A system structure identifier which can be achieved by using an unsupervised learning technique such as the Hebbian learning algorithm or the Kohonen's algorithm [14, 15] is employed to identify overall system operating conditions, which is to cover the whole range of operating application, not for the any fixed operation condition.

## 2.2. Control Loops

There are two kinds of control loops which are feedforward control loop and feedback control loop. In case of a feedforward control loop with multiple paths, it is hard to determine the state of final node to which each path from the starting node may have different effect.

Consider the digraph of figure 2 with  $A_i = +1$  as the fault origin and  $n$  paths from node  $A_i$  to node  $A_j$ .

Between two nodes  $A_i$  and  $A_j$ , a gain term  $g_k$  for each path is newly added to help determine the final state at node  $A_j$  which may be unknown yet due to the different fault propagation time and the sign on each path. There may be more than one path to determine the final state of the node  $A_j$  from the node

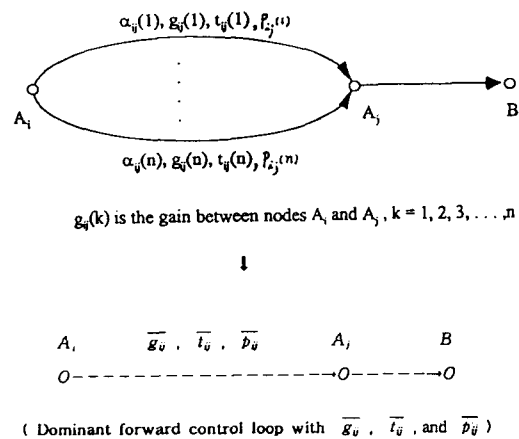


Fig. 2. Feedforward Control Loop with Multiple Paths

$A_j$ . Thus, suppose that  $g_{ij}$  as well as  $t_{ij}$  and  $\alpha_{ij}$  on each path is predetermined. Then, for  $N$  being the number of the survived paths from  $A_i$  to  $A_j$  which contribute to the determination of the final state of the node  $A_j$ , we can set  $\bar{g}_{ij}$  to be the total gain of the  $N$  survived paths as follows :

$$\bar{g}_{ij} = \sum_{k=1}^N (g_{ij}(k) \cdot \alpha_{ij}(k)) , \quad N \leq n \quad (4)$$

With  $\bar{g}_{ij}$ , we can estimate the final state of the node  $A_j$  by using the following equation in a quantitative manner :

$$\Delta A_j = \Delta A_i \cdot \bar{g}_{ij} \quad (5)$$

where

$$\Delta A = A_m - \bar{A}$$

and the resulting FPT  $\bar{t}_{ij}$  in this case is also estimated according to  $\bar{g}_{ij}$ , that is, the  $\bar{t}_{ij}$  can be the maximum FPT among  $N$   $t_{ij}$ s of  $N$  paths which affect the determination of  $\bar{g}_{ij}$ . The resulting FPP,  $\bar{p}_{ij}$ , can be obtained in the following equation,

$$\bar{p}_{ij} = \max_{i \in n} ( \min ( p_{ij}(i) , \bar{n}g_{ij}(i) ) ) \quad (6)$$

where  $\bar{n}g_{ij}$  is the normalized absolute gain value with maximum value of 1.

The relation (5) can be used to establish the final state of a node in a steady state or in a quasi-steady state condition. The transient or inter-state of the node  $A_j$  may also be determined by analyzing the behavior of the node  $A_i$  using  $g_{ij}$ ,  $t_{ij}$ ,  $\alpha_{ij}$ , and  $p_{ij}$  on each path.

For a feedback control loop with a single output, there are two operation modes in the control loop for the external disturbance. These are the normal loop working mode and the saturated mode. The saturated mode is for the case when the size of the disturbance exceeds the compensation capability of the loop. In case of internal faults of the control loop such as device faults, excessive setpoint change, or disturbance, etc., there is no more compensating capability available within the control loop, and the control loop becomes an ordinary digraph.

In general, if the feedback control loop is influenced by an excessive external disturbance or fault, it fails to compensate for the disturbance. In this case, the compensating feedback path does not function any longer and only feedforward path(s) remains in operation. If the feedback control loop maintains its normal control capability against the external influence, then the controlled variable and its related variables do not appear via control action within the control loop. In case of fault(s) within the feedback control loop, the feedback control loop becomes an ordinary digraph and it is not a control loop any more.

### 3. Training Data Extraction

It is very important to get reliable training data to describe the system behavior fairly well even though data are formed based on a system model, not based on the expert knowledge. It is also desirable to explain the extracted data flow including the routes of fault propagation. The SDG model described in the previous section is used as a systematic fault model for generating training data for the fault diagnosis in this work.

#### 3.1. Steady-state or Quasi-steady-state Case

It is quite difficult to locate the fault origin exactly, especially when the abnormal signals grow exponentially and appear for a short time, because the abnormal states in the process are often detected at devices other than the failed device itself. When a fault exists in the form of positive fault ('+') or negative fault('-') in the SDG, the fault can propagate into the adjacent nodes in the arrow directions with the sign influence on each branch connected to the fault source until the affected sensors exhibit the prescribed corresponding symptoms.

Under the assumption that when a node generates a fault, the other nodes in the SDG remain normal, the procedure to get the symptom patterns of sensor

s for the training data of a subsystem is given as follows:

- 1) Draw a SDG for the subsystem. The readings of sensors are transformed into some continuous values using Eq. (2).
- 2) Mark with the superscript of asterisk the first nodes that are connected to the nodes of the adjacent subsystems. These marked nodes will be utilized for the system-wise faults diagnosis later in section 4.
- 3) Convert the feedforward loop with multiple paths into the digraph with dominant path with  $\bar{g}_{ij}$ ,  $\bar{t}_{ij}$ , and  $\bar{p}_{ij}$  using Eqs. (5)&(6).
- 4) Select one process device node with "source node = '+1'" as the fault origin, the total influence from the source node to all the affected sensor nodes is calculated as follows:

The state of a sensor node = The state of a source node  $\cdot \bar{sign} \cdot \bar{FPT}$

where  $\bar{sign}$  and  $\bar{FPT}$  are the total sign and the total FPT which are obtained by multiplying all signs and all FPTs along the path from the source node to the sensor node respectively.

- 5) Put the total influence which is  $\bar{sign} \cdot \bar{FPT}$  between the source node and all the affected sensor nodes. The '0' means that the selected source node does not affect the corresponding sensor node.
- 6) Repeat step 4) and step 5) for the rest of the nodes of process devices within the subsystem including the sensor itself. Finally, the relationship between causes as source nodes and consequences as the corresponding sensor patterns is obtained in a table called "cause and consequence table".
- 7) Put the same patterns into one group and obtain the reduced cause and consequence table. This reduced table is used for training the ANN for the fault diagnosis of the subsystem.
- 8) Repeat the whole procedure from step 4) to step 7) in case each source node = '-1'.

It is remarked that some physical parameters such

as flow and pressure can not propagate any further when a valve along the path is closed due to high or low predetermined setpoints. In this case, we can generate two types of sensor patterns-the valve open case and the valve close case.

### 3.2. Transient Case

In order to train an ANN for the fault diagnosis under a transient, we need a large time-dependent data of sensors which represent the trace of each fault propagating into sensors with time. There can be different symptoms of sensors, which reflects the degree of influence propagated from a fault as time passes by, but it not easy to get transient data for every possible fault case in the real plant.

If the fault propagation time on each branch is obtained as stated in section 2, we can generate the sensor patterns from each fault origin under a transient condition from the time differences arriving at each sensor from a fault origin. It is done by using the information on the fault propagation times along the corresponding paths. There may be more than one sensor pattern before settling to the steady-state depending on the sequence of the symptoms of sensors from a propagated fault. In most practical cases, it is very difficult to calculate the exact value of FPT, rather each FPT value can be considered as a value in a fuzzy sense.

A fuzzy variable, which is defined as a convex normalized fuzzy set of the real line by Zimmermann (1985)[16] is introduced to depict an uncertain FPT from node  $x_i$  to node  $x_j$ ,  $\widetilde{t}_{ij}$ . The  $\widetilde{t}_{ij}$  can be represented as a discrete summation form or a continuous integral form such as bell-type and triangular-type.

If there exist  $(m+1)$  branches by nodes  $x_{p1}$ ,  $x_{p2}$ , ...,  $x_{pm}$  along a path from node  $x_i$  to node  $x_j$ , then the FPT  $\widetilde{t}_{ij}$  is calculated as follows:

$$\widetilde{t}_{ij} = \widetilde{t}_{i p_1} \oplus \widetilde{t}_{p_1 p_2} \oplus \cdots \oplus \widetilde{t}_{p_m j} \quad (7)$$

where  $\oplus$  is a fuzzy addition operator. In this way we can derive every fuzzy FPT from a faulty source node

to every affected final sensor node.

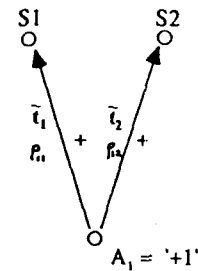
For instance, considering figure 3 with bell-type fuzzy FPTs  $\tilde{t}_1$  and  $\tilde{t}_2$  respectively which are obtained as described above, the inter-state pattern(s) can be assigned as shown in table I according to the time difference  $\Delta t'$  between two FPTs  $t'_1$  and  $t'_2$  which are  $\alpha$ -cut points of membership functions  $\tilde{\mu}_{t1}$  and  $\tilde{\mu}_{t2}$  respectively. Simply, as the point  $p$  which is the maximum point of  $\tilde{\mu}_{t1} \cap \tilde{\mu}_{t2}$  in figure 3 draws near to the peak point of  $\tilde{\mu}_{t1} = \tilde{\mu}_{t2}$ , the inter-state pattern approach to the pattern  $(S_1, S_2) = (+P_{11}, +P_{12})$  while as the point  $p$  reach a minimum point of zero which also includes a point of larger  $\Delta t'$ , the inter-state pattern goes near to the point of  $(S_1, S_2) = (+P_{11}, 0.0)$  and there may exist more than one inter-state sensor pattern with the consideration of the transient behavior of the plant if the  $\Delta t'$  is much larger than the system sampling time and  $\alpha$ -cut points are determined accordingly.

The procedure is identical with the steady-state case except for the insertion of the inter-state pattern(s) of sensors during the transient for each source node. In this case, if any feedforward or feedback control loop is involved along the paths from a fault node to the affected sensors, we should be careful in deciding inter-state patterns among sensors because the behavior of the control loop may be undetermined in transient.

For the feedback control loop, the controlled variable, especially in case of an abruptly excessive set-point change, may take an inter-state before settling to a steady-state. The inter-state can be obtained by the process operating data or by the simulation using the fault propagation time and the gain on each branch of the feedback control loop or by the model of the control system.

#### 4. Fault Diagnosis

Once the reduced sensor patterns are acquired from the SDG model by using the data extraction method, they are used to train the artificial neural



$t$  : time variable

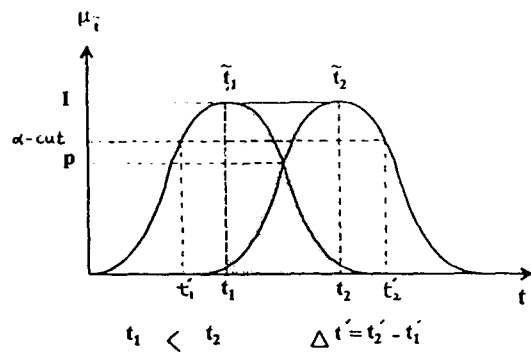


Fig. 3. Fuzzy FPTs  $\tilde{t}_1$   $\tilde{t}_2$

network(ANN) that runs based on the error back-propagation algorithm[15]. Specifically, the fault diagnosis is performed as follows. First, the incipient faults are diagnosed by recalling the pre-trained ANN constructed for at each subsystem, and then the spurious faults due to the physical relationship among the subsystems are removed at the second stage using inter-related knowledge among the divided subsystems and the time sequence of faults-occurrence of each subsystem as shown in figure 1. The fault rate of process device (fault candidate) and total FPP from each candidate of fault origin are used to select the most probable fault origin from more than one fault origin candidates at each neural network. Furthermore, the adoption of SDG as a physical model can render the explanation of diagnosis results as does in a conventional expert system.

#### 4.1. Incipient Faults Diagnosis

The reading of each sensor node is converted into a normalized value using Eq. (2) in a continuous form rather than in a discrete value. The converted continuous value of each sensor is utilized as the input to the neural network. The faults diagnosis procedure for a typical subsystem is as follows:

- (1) Train the corresponding ANN using the obtained "reduced table" as the input-output patterns.
- (2) Based on the trained ANN for the subsystem to be diagnosed, the diagnoses of the faults of process devices and the troubled pipe(s) are performed for the converted values of newly sensed values.

If there exist several candidates for a fault origin, ordering of the candidates is performed to select the most suspected fault origin, based on the fault rate of each candidate and total FPP from each candidate to any sensor within the corresponding sensor pattern; that is, the candidates are ranked according to the fault rates multiplied by total FPPs.

It is quite tedious to train the ANN for the combinatorially large number of patterns resulting from multiple faulty nodes. However, we can observe that the network trained on a single fault has the ability to diagnose multiple faults due to the nonlinear mapping capability of the network[6]. It is remarked that the noise from a sensor is also filtered out due to noise-tolerance capability[13, 14]. Multiple faults in this paper refer to the collected faults which may be occurred in more than one subsystem simultaneously as well as multiple faults existing in one subsystem.

#### 4.2. Removal of Spurious Faults(RSF)

As mentioned in section 2.1, the spurious faults should be identified and removed. Since the divided subsystems may be physically inter-related and the fault diagnosis is performed at each subsystem independently as noted earlier, a fault or faults in a sub-

system can propagate to the adjacent subsystems and such subsystems are called "fault-affected subsystems". Of course, we should not exclude the possibility of real faults occurred within the fault-affected subsystems. It is assumed, however, that nodes marked with superscript of asterisk are not the real faulty nodes when they are affected from the faults of the other subsystems.

Based on (1) the independence in fault(s) diagnosis on each subsystem base, (2) the inter-related knowledge about nodes marked with superscript of asterisk connecting the adjacent subsystem(s), and (3) the time information of fault(s) occurrence of each faulty subsystem, the method of removing the spurious faults is described as below:

- 1) Select the first fault-occurred subsystem.
- 2) Collect the set  $F_s$  of faults and the set  $F_s^*$  of the nodes marked with superscript of asterisk of the selected subsystem.
- 3) Calculate the intersection  $I_s = F_s \cap F_s^*$ . The elements of set  $I_s$  are the nodes which are declared as the fault-nodes marked with the superscript of asterisk.
- 4) Find the external subsystems which are connected to any element of the set  $I_s$ .
- 5) Choose the set  $F_{ex}$  of the faults detected in all external subsystems which are found in step 4).
- 6) Select the set  $F_{ex}^*$  of elements from the set  $F_{ex}$ , which are directly connected to any element of the set  $I_s$  through any unbroken path with non-zero FPP.
- 7) Select one element  $a_i^* \in I_s$ ,  $i \in \mathbb{I}$ (integer) and collect the set  $\{a_i^*\}$  of the nodes by back-tracing along the paths starting from the node  $a_i^*$  and going back to the elements of the set  $F_{ex}^*$ .
- 8) Calculate the intersection  $S = \{a_i^*\} \cap F_{ex}^*$ .

If  $S = \emptyset$  the node  $a_i^*$  is not the spurious fault, and goto step 9).

Here  $\emptyset$  denotes the empty set.

If  $S \neq \emptyset$  the node  $a_i^*$  is the spurious fault so that



this node  $a_i^*$  is removed from the set  $F_s$ .

9) Repeat the procedure step 8) for the rest of elements of the set  $I_s$ .

10) Repeat the procedure from step 2) to step 9) for the rest of the subsystems in the time sequence of the fault-occurrence.

The above procedure essentially means that, for each subsystem selected, the nodes marked with the superscript of asterisk are removed from the declared faults candidates if they are influenced from the fault-nodes of the related external subsystems. Figures 4 and 5 show the overall algorithm for the proposed method.

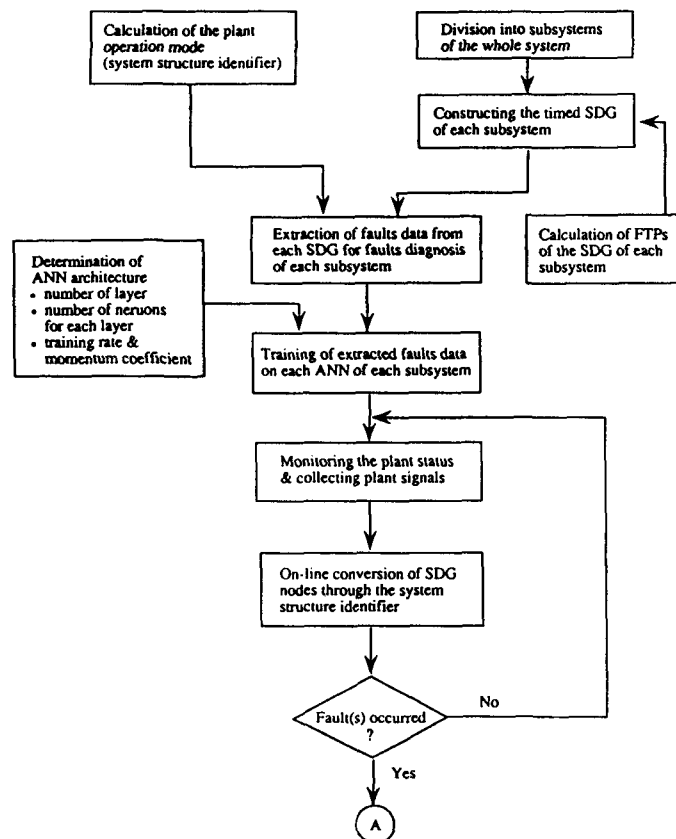
### 5. Application and Results

This method is applied for diagnosis of a primary

side in the Kori nuclear power plant unit 2 in Korea under a transient condition with an unit value of FPP on each branch of the SDG model.

The digraphs of the pressurizer and its connected systems are drawn with arrows according to their cause-effect relations as shown in figure 6 and the names of nodes are listed in Table 2.

The normal and alarm setpoint values of each sensor of the pressurizer are presented in Table 3. Each threshold value is determined based on the degree that the operator can be aware of the abnormal state of each sensor according to the plant characteristics and the operation condition. The fault patterns of each component of the pressurizer are shown in Table 4 in case each source node = '+1', which is made through the method derived in section 3, the analysis of the plant operation data, and the simulation from the FISA-2/WS system simulator which is



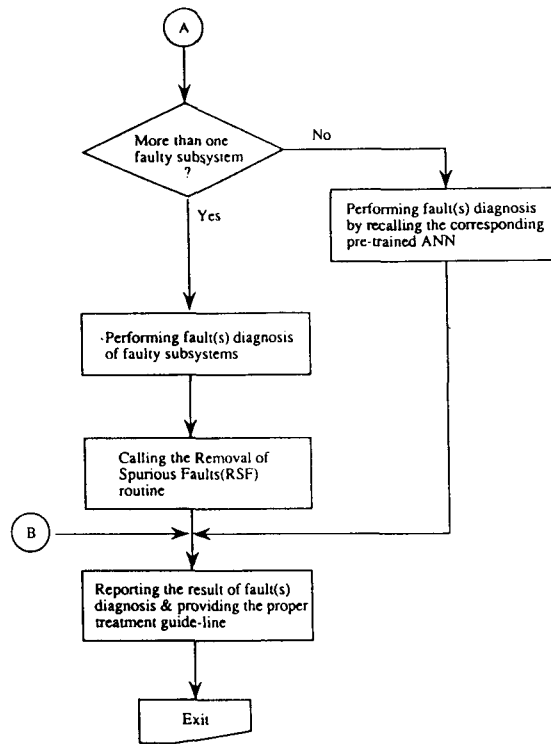


Fig. 4. Overall Algorithm of the Methodology

Table 1. Sensor Patterns of Figure 3

Sensor patterns		Source node
$S_1$	$S_2$	$A_1 = +1.0'$
$+P_{11}$	0.0	Shortly after $t_1'$
$+P_{11}$	@ $*P_{12}$	$t_1' < t < t_2'$ (inter-state)
$+P_{11}$	$+P_{12}$	after $t_2'$

@ : a value between 0 and +1

developed in Korea Advanced Institute of Science and Technology(KAIST) and verified with RETRAN-2 and RELAP5/MOD3 codes. The fault pattern of a component is more than one since the transient case as well as the steady-state case is considered. For example, the fault patterns of power operated relief valve(PORV) 1 or 2 leaking inadvertently are the following three patterns in Table 4; (1) the first pattern is appeared before the effect is reac-

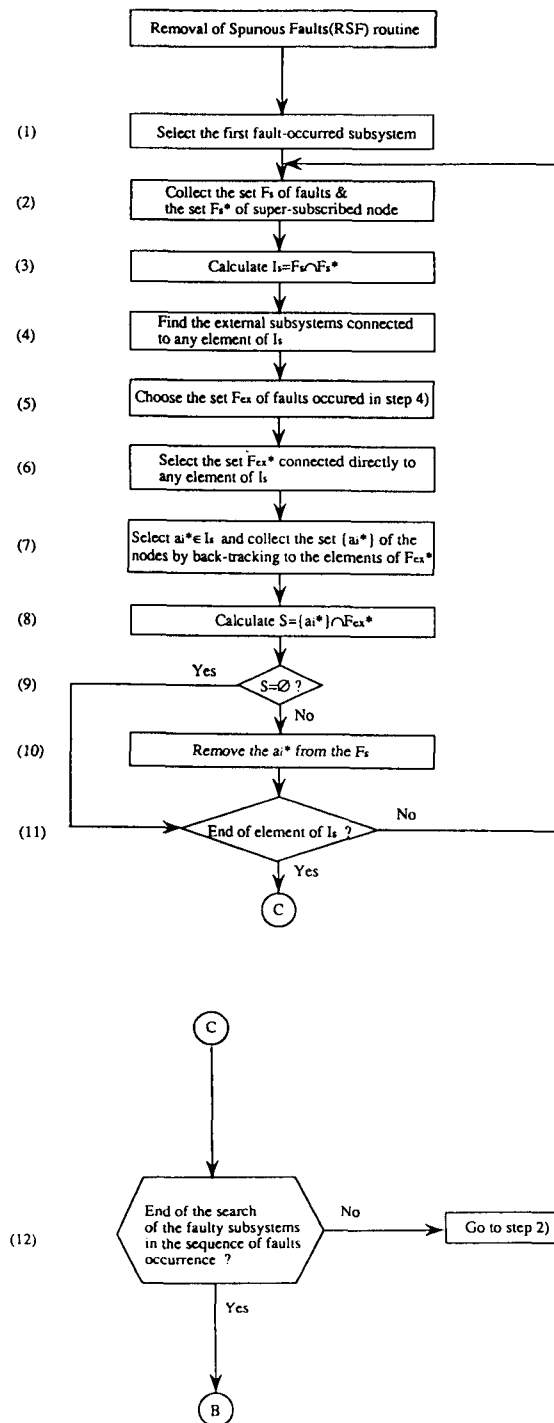


Fig. 5. Removal of Spurious Faults Routine

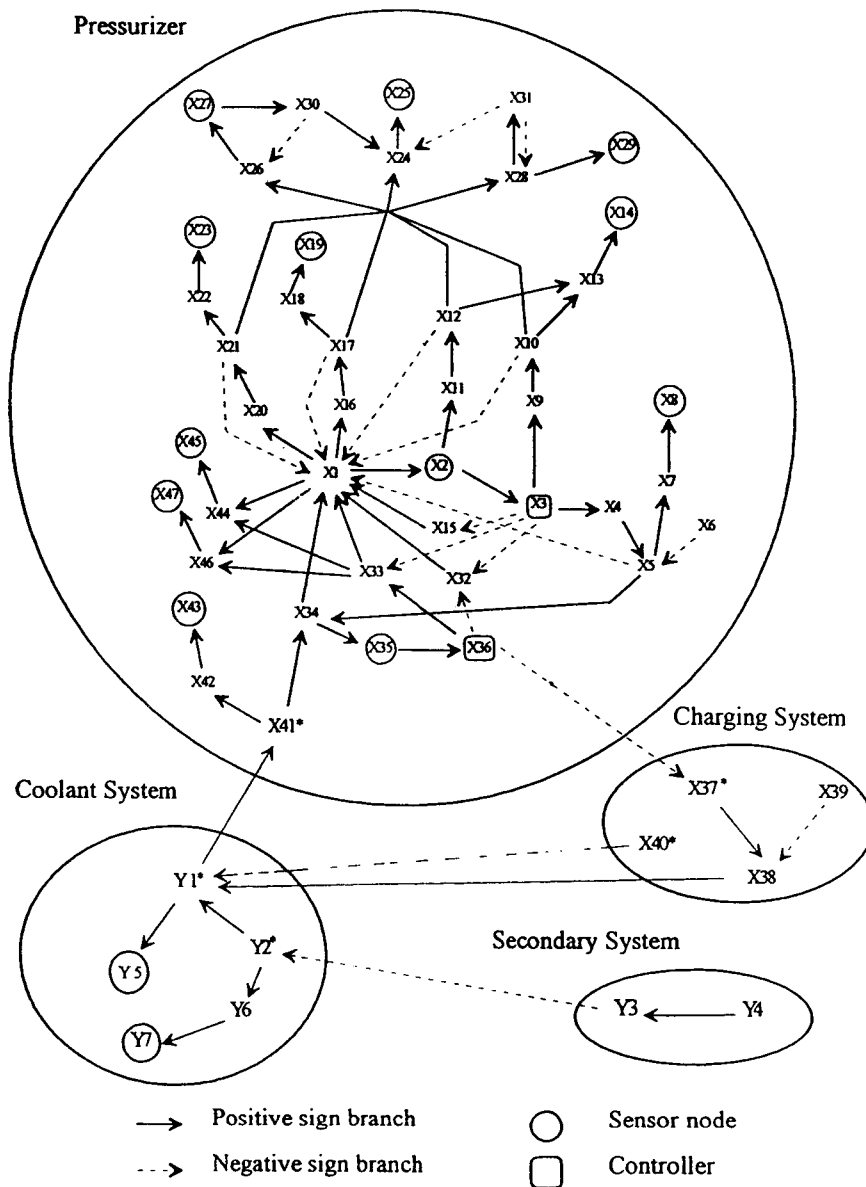


Fig. 6. Digraph of the Pressurizer and its Connected Systems

hed to the relief tank, (2) the second pattern shows the state when the fault is spread to the relief tank, and (3) the third pattern is for the state when the pressure and water level can be controlled because the value of leakage flow is little. The patterns of two PORV faults are the same because there is only one temperature sensor that indicates the condition of

the opening of two valves.

The fault patterns are trained using the back-propagation method which is one of the supervised learning method of the neural networks. The network is composed with input layer(12 nodes), hidden layer (65 nodes), and output layer(26 nodes). The number of nodes in each layer is determined by computer

Table 2. The Names of Nodes in Figure 6.

NODE	NAME	NODE	NAME
X <sub>1</sub>	Pressure	X <sub>28</sub>	PRT Pressure
X <sub>2</sub>	Pressure Sensor	X <sub>29</sub>	PRT Pressure Sensor
X <sub>3</sub>	Pressure Controller	X <sub>30</sub>	PRT Coolant
X <sub>4</sub>	spray Valve	X <sub>31</sub>	Rupture Disc
X <sub>5</sub>	Spray Line Flow	X <sub>32</sub>	Proportional Heater
X <sub>6</sub>	Spray Line Tube	X <sub>33</sub>	Backup Heater
X <sub>7</sub>	Spray Line Temp	X <sub>34</sub>	Level
X <sub>8</sub>	Spray Line Temp Sensor	X <sub>35</sub>	Level Sensor
X <sub>9</sub>	PORV1	X <sub>36</sub>	Level Controller
X <sub>10</sub>	PORV1 Line Flow	X <sub>37</sub>	Charging Valve
X <sub>11</sub>	PORV2	X <sub>38</sub>	Charging Flow
X <sub>12</sub>	PORV2 Line Flow	X <sub>39</sub>	Charging Line Tube
X <sub>13</sub>	PORV Temp.	X <sub>40</sub>	Let down Valve
X <sub>14</sub>	PORV Temp. Sensor	X <sub>41</sub>	Surge Flow
X <sub>15</sub>	PORV Interlock Valve	X <sub>42</sub>	Surge Line Temp.
X <sub>16</sub>	SRV1	X <sub>43</sub>	Surge Line Temp. Sensor
X <sub>17</sub>	SRV1 Flow	X <sub>44</sub>	Water Temp.
X <sub>18</sub>	SOV1 Line Temp.	X <sub>45</sub>	Water Temp. Sensor
X <sub>19</sub>	SRV1 Line Temp Sensor	X <sub>46</sub>	Vapor Temp.
X <sub>20</sub>	SRV2	X <sub>47</sub>	Vapor Temp. Sensor
X <sub>21</sub>	SRV2 Flow	X <sub>1</sub>	Pressure of Coolant System
X <sub>22</sub>	SRV2 Line Temp.	X <sub>2</sub>	Heat of Collant System
X <sub>23</sub>	SRV2 Line Temp. Sensor	X <sub>3</sub>	Heat of Secondary System
X <sub>24</sub>	Pressurizer Relief Tank(PRT) Level	X <sub>4</sub>	Turbine Load
X <sub>25</sub>	PRT Level Sensor	X <sub>5</sub>	Pressure Sensor of Coolant
X <sub>26</sub>	PRT Temp.	X <sub>6</sub>	Temp. of Coolant
X <sub>27</sub>	PRT Temp. Sensor	X <sub>7</sub>	Temp. Sensor of Coolant

experiments designed to minimize computational time and achieve suitable classification. The faults diagnosis results such as PORV leakage(the second pattern), spray valve over-opening(the 4th pattern), safety relief valve 1(SRV1) leakage(the 10th pattern), and surge flow into the pressurizer(the 34th pattern) are shown in Table 5. The diagnosis results of the noise patterns are shown in Table 6. Here, the noise patterns are not realistic but are generated artificially within 10% in magnitude of the normalized value of each sensor to verify the sensor noise filtering capability of the ANN because there is very little noise on the sensors at the real plant site. As shown in Tables 5 and 6, the method using the ANN can find the

faults fast and exactly. It is also possible to use this method to diagnose the faults of sensors themselves because their patterns can also be made and trained (refer to the patterns of the 22th to the 27th row and the patterns of the 29th to the 32th row in Table 4).

The algorithm of the system-wise fault diagnosis is applied to the case of decreasing turbine load. When it occurs, the heat removal by the secondary feedwater is decreased in the steam generator and the surge flow resulted from increased pressure of the coolant system is streamed into the pressurizer. The water level and the pressure of the pressurizer are increased and the fault is propagated to other devices of the

**Table 3. Sensor Data of Kori Nuclear Power Plant unit 2**

Node	Normal Value	Alarm Setpoint		Threshold Value
		High	Low	
2	2235	2310	2185	20
8	536		532.4	2
14	86	105.8		10
19	86	105.8		10
23	86	105.8		10
25	75	85	54	3
27	100	127		10
29	14.7	23.23		5
** 35	60	+5	-5	2
43	615.4		532.4	10
45	651.7	656.6		3
47	651.7	656.6		3

♣ Units are as follows :

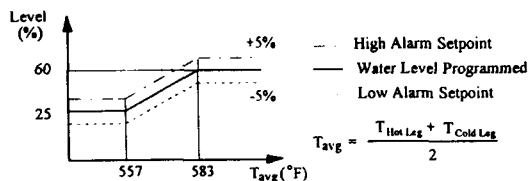
Nodes 2, and 29 (Pressure) : psia

Nodes 8, 14, 19, 23, 27, 43, 45, and 47

(Temperature) : °F

Nodes 25, and 35 (Water Level) : %

\*\* Pressurizer Water Level : Function of Average Temperature of the Coolant System



pressurizer as depicted in figure 12. The decreasing turbine load, therefore, causes the pressurizer to be seen as failed. If the ANN is applied for the subsystem diagnosis when the turbine load is decreasing, the set  $F_s$  of the pressurizer faults is  $\{X_{41}\}$  whose fault generates the 34th pattern in Table 5. The fault  $X_{41}$  is affected by  $Y_1$  of the coolant system (see figure 6). The fault  $X_{41}$ , therefore, is deleted from the set  $F_s$  and the original fault is not detected in the pressurizer. If the method is applied to the coolant system, the set  $F_s$  of the subsystem is  $\{Y_2\}$ . The fault  $Y_2$ , however, is also deleted from set the  $F_s$  of the coolant system because the fault is affected from the secondary system. Finally, the fault  $Y_4$ , turbine load decreases,

is detected in the secondary system. The procedure discussed in section 4.2 for this case is as follows: (1) the pressurizer is selected as the first fault-occurred subsystem, (2)  $F_s = \{X_{41}\}$  and  $F_s^* = \{X_{41}\}$ , (3)  $I_s = \{X_{41}\}$ , (4) external subsystem is the coolant system, (5)  $F_{ex} = \{Y_2\}$ , (6)  $F_{ex}^* = \{Y_2\}$ , (7)  $\{X_{41}\}^* = \{Y_1, Y_2\}$ , (8)  $S = \{Y_2\}$ . Therefore,  $X_{41}$  is removed from the set  $F_s$ , and the faults are not discovered in the pressurizer. By applying the above procedure to other subsystems, the real fault of this situation is found to be fault  $Y_4$  (turbine load decreasing) in the end.

## 6. Conclusions

An improved method based on Chung's approach in 1994 [1] for incipient multi-fault diagnosis in real time is proposed and applied to the real plant. Some of the merits of the method are: (1) it is capable of incipient multiple fault diagnosis of large-scale systems in real time because the fault diagnosis of a large-scale system is performed by the diagnosis of subsystems using the distributed artificial neural networks and a knowledge-based system, (2) the method shows more practical applicability because the fault diagnosis is performed not only in steady-state but also in transient-state cases using fuzzy FPT and FPP on each branch of the SDG model, (3) due to the use of the physical fault model (SDG model), the result of the fault diagnosis can be explained in a highly reliable manner, (4) if there exist several candidates for a fault origin, ordering of the candidates is performed to select the most suspected fault origin, based on the fault rate of each candidate and total FPP from each candidate to any sensor within the corresponding sensor pattern; that is, the candidates are ranked according to the fault rates multiplied by total FPPs, which gives more reliable result on selecting fault origin, and (5) this may be used over the whole system operating range, not at a fixed operating range via the system structure identifier.



Table 5. The Results of the Pattern 2, 4, 10, 34

(b) Output

	Pattern 2	Pattern 4	Pattern 10	Pattern 34		Patten 2	Patten 4
$X_9$	<b>0.993979</b>	0.002106	0.000000	0.000214	$X_9$	<b>0.991639</b>	0.007183
$X_{11}$	0.993130	0.001813	0.000000	0.000342	$X_{11}$	<b>0.990631</b>	0.005863
$X_{16}$	0.007138	<b>0.996342</b>	0.000000	0.000004	$X_{16}$	0.012563	<b>0.990244</b>
$X_{20}$	0.004411	0.002270	0.000000	0.000001	$X_{20}$	0.001867	<b>0.006677</b>
$X_{32}$	0.000517	0.000000	<b>0.995545</b>	0.007061	$X_{32}$	0.000599	0.000000
$X_{33}$	0.000095	0.000000	<b>0.988018</b>	0.000462	$X_{33}$	0.000195	0.000000
$X_4$	0.000955	0.003752	0.000001	0.000000	$X_4$	0.001421	0.002231
$X_6$	0.000000	0.000000	<b>0.985692</b>	0.000002	$X_6$	0.000000	0.000000
$X_{31}$	0.000000	0.000132	0.000765	0.000000	$X_{31}$	0.000000	0.000101
$X_{37}$	0.000033	0.000000	0.003957	0.010687	$X_{37}$	0.000086	0.000000
$X_{39}$	0.000011	0.018644	0.000001	0.000000	$X_{39}$	0.000005	0.023867
$X_2$	0.000000	0.000000	<b>0.999923</b>	0.001681	$X_2$	0.000000	0.000000
$X_{35}$	0.000000	0.000000	0.001272	0.000294	$X_{35}$	0.000000	0.000000
$X_8$	0.000000	0.000550	0.004036	0.000001	$X_8$	0.000000	0.000285
$X_{14}$	0.000174	0.000000	0.002581	0.000149	$X_{14}$	0.000241	0.000000
$X_{19}$	0.000000	0.006442	0.003576	0.000000	$X_{19}$	0.000001	0.001108
$X_{23}$	0.000000	0.000001	0.004160	0.000001	$X_{23}$	0.000000	0.000001
$X_{25}$	0.000274	0.003461	0.001597	0.000045	$X_{25}$	0.000319	0.001927
$X_{27}$	0.000111	0.000605	0.000769	0.000002	$X_{27}$	0.000040	0.000531
$X_{29}$	0.000412	0.001363	0.000822	0.000046	$X_{29}$	0.000702	0.000602
$X_{43}$	0.001598	0.000476	0.006473	0.006823	$X_{43}$	0.002215	0.000410
$X_{45}$	0.000018	0.001337	0.000095	0.000000	$X_{45}$	0.000021	0.001172
$X_{47}$	0.000035	0.002787	0.000021	0.000002	$X_{47}$	0.000037	0.002432
$X_3$	0.001989	0.008432	0.000000	0.000000	$X_3$	0.001289	0.010711
$X_{36}$	0.000000	0.000000	0.002951	0.000000	$X_{36}$	0.000000	0.000000
$X_{41}$	0.005512	0.000000	0.000003	<b>0.989672</b>	$X_{41}$	0.030179	0.000000

Table 6. The Results of the Patterns with Noise

(a) Input Patterns

Input	$X_2$	$X_8$	$X_{14}$	$X_{19}$	$X_{23}$	$X_{25}$	$X_{27}$	$X_{29}$	$X_{35}$	$X_{43}$	$X_{45}$	$X_{47}$
Pattern 2	-0.9	0.1	1.1	0.1	0.0	0.95	0.9	1.1	1.05	0.05	0.1	0.0
Pattern 4	-1.1	0.0	0.1	0.9	0.1	0.01	0.1	0.0	0.0	0.05	0.02	0.1

## Nomenclature

 $A_m$  measured value of A $\bar{A}$  nominal value of A $A_i, X_i$  nodes  $A_i$  and  $X_i$  $A_s$  threshold value of A $\Delta A$  measured value of A - nominal value of A

N number of the survived paths in feedforward control loop

$S_i$	sensor $i$
$Z_i$	state variable $i$
digraph	directed graph
$g_{ij}$	gain factor from node $i$ to node $j$
$\overline{g_{ij}}$	total gain factor from node $i$ to node $j$ in multi-path feedforward control
$n$	total number of forward paths in feedforward control loop
$\overline{ng_{ij}}$	the normalized absolute gain value with maximum value of 1 along a path from node $i$ to node $j$ .
$p$	maximum point of $\tilde{\mu}_{i1} \cap \tilde{\mu}_{i2}$
$p_{ij}$	fault propagation probability from node $i$ to node $j$
$\overline{sign}$	the total sign which is obtained by multiplying all signs along the path from the source node to the final sensor node.
$\overline{FPT}$	the total FPT which is obtained by multiplying all FPTs along the path from the source node to the final sensor node
$t_1$	FPT at maximum value of $\tilde{t}_1$
$t_2$	FPT at maximum value of $\tilde{t}_2$
$\tilde{t}_1$	fuzzy variable of $t_{12}$
$\tilde{t}_2$	fuzzy variable of $t_{11}$
$t_{ij}$	fault propagation time from node $i$ to node $j$
$\tilde{t}_{ij}$	fuzzy fault propagation time from node $i$ to node $j$
$\overline{t_{ij}}$	total FPT from node $i$ to node $j$ in multi-path feedforward control loop
$\Delta t$	time difference between $t_1$ and $t_2$
$\alpha_{ij}$	sign of the arrow from node $i$ to node $j$
$\phi$	empty set

### References

1. Hak-Yeong Chung and Zeungnam Bien, "Incipient Multiple Fault Diagnosis in Real Time with Application to Large-Scale Systems", *IEEE TNS* Vol. 41, NO. 4, August. 1692–1703 (1994)
2. Kajiyo Watanabe, Liya Hou, "An Optimal Neural Network for Diagnosing Multiple Faults in Chemical Processes", *IECON'92 International Conference on Industrial Electronics, Control, Instrumentation, and Control*. 1068–1073 (1992)
3. Cheng-Ching Yu and Chyuan Lee, "Fault Diagnosis Based on Qualitative/Quantitative Process Knowledge", *AIChE J.*, vol. 37, No. 4. 617–628 (1991)
4. T. Sorsa, Heikki N., No Koivo, and H. Koivisto, "Neural networks in process fault diagnosis", *IEEE Trans. on systems, man, and cybernetics*, Vol. 21, No. 4. 815–825 (1991)
5. J.C. Hoskins, K.M. Kaliyur, and David M. Himmelblau, "Fault diagnosis in complex chemical plants using artificial neural networks", *AIChE Vol. 37*. 137–141 (1991)
6. V. Venkatasubramanian, R. Vaidyanathan, and Y. Yamamoto, "Process fault detection and diagnosis using neural networks-steady-state process", *Computers Chem. Engng.* Vol. 14, No. 7. 699–712 (1990)
7. D.Q. Qian, "An improved method for fault location of chemical plants", *Computers Chem. Engng.* Vol. 14, No. 1. 41–48 (1990)
8. M.A. Kramer, and J.A. Leonard, "Diagnosis using backpropagation neural networks-Analysis and criticism", *Computers Chem. Engng.* Vol. 14, No. 12. 1323–1338 (1990)
9. Chung-Chien Chang, and Cheng-Ching Yu, "On-line fault diagnosis using the signed directed graph", *Ind. Engng. Chem. Res.* 29. 1290–1299 (1990)
10. M.A. Kramer, and B.L. Palowitch, Jr. "Arule-based approach to fault diagnosis using the signed directed graph", *AIChE J.*, Vol. 33, No. 7 (1987), 1067–1078.
11. R. Isermann, "Process fault detection based on modeling and estimation method-a survey", *Automatica*. 20. 387 (1984)
12. M. Kokawa, S. Miyazaki, and S. Shingai, "Fault location using digraph and inverse direction search with application", *Automatica*, Vol. 19, No. 6. 729–735 (1983)



13. D.E. Rumelhart and J.L. McClelland, *Parallel Distributed Processing*, Vol. 1, Cambridge, MA:MIT Press (1987)
14. Y.H. Pao, *Adaptive Pattern Recognition and Neural Network*, New York: Addison-Wesley (1989)
15. Philip D. Wasserman, *Neural Computing-theory and practice*, Van Nostrand Reinhold (1989)
16. H. -j. Zimmermann, *Fuzzy Set Theory and its Applications*(Kluwer-Nijhoff Publishing, New York (1985)